STUDY ON THE AERODYNAMIC CHARACTERISTICS OF HIGH-ALTITUDE PROPELLERS WITH PROPLETS

Xudong Yang, Jianhua Xu, Bo Wang, Chao Song, Shunlei Zhang
School of Aeronautics, Northwestern Polytechnical University, Xi'an, China

Keywords: *High-Altitude Propeller; Proplet; Low Reynolds Number; Efficiency Improvement*

Abstract

Propeller is the main part of the high-altitude airship propulsion system. Its performance, especially its efficiency, has great effect on the overall design of the airship at low Reynolds numbers. Based on the original design of high-altitude propeller, this paper attempts to improve its aerodynamic efficiency by adding proplets. Reynolds averaged Navier-Stokes equations are used to examine the impact of the proplets on the efficiency and aerodynamic performance of the propeller. On the other hand, to compare the aerodynamic performance of propellers with the same power, a method based on Newton Iteration is proposed, which can adjust rotation speed automatically and efficiently. The results show that the incident angle of the proplet has dominant effects on the efficiency of propellers. In the compressible flow, it should not be larger than 5 degrees. Bending radius can improve the efficiency obviously, only when it exceeds 2%R. It also helps to improve the efficiency when the bending angle is close to 90 degrees. In addition, the sweep angles of proplet are found to show negligible impact on the efficiency of propellers in the incompressible flow, but improve the efficiency of propellers considerably in the compressible flow. The larger the sweep angle, the higher the efficiency.

1 General Introduction

In order to meet the long-time spot hovering demand of high-altitude airships and long-endurance unmanned aerial vehicles, it has become a key problem to improve the efficiency of propellers. However, it can be very difficult to improve the efficiency of high-altitude propellers under the influence of the low Reynolds number of the flow, for the nonlinear aerodynamic characteristics caused by laminar separation. Hence, considering the constraints of the diameter and blade manufacturing, etc., it is difficult to meet the requirements of the aerodynamic efficiency by conventional propellers configuration. On the other hand, other complex flow control techniques, such as co-flow jet flow control [1][2], plasma[3], etc., are too complicated to manufacture in practice in the near future. Consequently, in this article, proplets are introduced to improve the aerodynamic efficiency.

In 1970s, Whitcomb, R.T., introduced winglets to reduce the induced drag of the wing and to weaken the wake of large aircrafts. Because of their simple structure and obvious aerodynamic effects, they have also been applied to aviation propellers. In 1980, Irwin, K. and Mutzman, R. [4] studied the potential of the proplets to improve the efficiency using the vortex theoretical and experimental methods. They concluded that the proplets could improve the efficiency of the propellers by about 1%, and the improvement was related to the height of the proplets. In 1984, Chang and Sullivan [5] used the vortex lattice method to optimize the section twist angles of propellers, including the twist angles of the proplets. The result showed that the proplets could improve the efficiency of the propeller by 1%-6%, compared with the baseline aerodynamic configuration. In 1989, Valarezo[6] introduced the proplets to the air-craft propeller in high subsonic cruise flows (M=0.8). In 2006, Sullivan [7] firstly introduced the proplets to the model airplane propellers, and their theoretical

analysis showed that proplets could improve the aerodynamic efficiency of the propeller up to 10%, although the experimental results were not discernable. Recently, our research team studied the aerodynamics performance of the near space propellers with proplets [8][9]. Based on the previous research, this article systematically examines the impact of the key parameters of proplets on the aerodynamic efficiency of propellers in order to improve aerodynamic efficiency of high-altitude propellers.

2 Computational Methods

In order to resolve the detailed tip vortex structure of the propellers, an in-house code named ROTNS [10][11], based on the RANS (Reynolds Averaged Navier-Stokes) equations, is used. In addition, the chimera grid technology is adopted to generate the grid and to facilitate the implementation of the periodic boundary conditions.

2.1 Governing equations

When the flow velocity is perpendicular to the propeller disk, the flow is quasi-steady in the rotating frame fixed on the propeller. The equations in integral form can be written as follows:

$$\frac{\partial}{\partial t}\iiint_{\Omega}\mathbf{W}dV+\iint_{\partial\Omega}\mathbf{H}\cdot\mathbf{n}dS-\beta\iint_{\partial\Omega}\mathbf{H}_{v}\cdot\mathbf{n}dS+\iiint_{\Omega}\mathbf{G}dV=0 \qquad (1)$$

where $\mathbf{W}=[\rho,\rho u,\rho v,\rho w,\rho E]^{T}$

ρ, u, v, w and E denote the density, the three components of the fluid velocity vector in the Cartesian coordinates, and the total energy per unit mass, respectively. $\mathbf{H}$ and $\mathbf{H}_v$ are the inviscid flux vector and the viscous flux vector, respectively. Ω, S, $\mathbf{n}$ are the volume, the surface area and the unit-normal outer vector of the control volume, respectively. When the β equals to one, the governing equations are the N-S equations, and when the β equals zero, the governing equations reduce to the Euler equations.

The cell-centered finite-volume method is used to solve the governing equations. The cell-centered scheme [12] is used for space discretization while the LU-SGS implicit scheme [13] is used for time advancement. The B-L turbulence model [14] is adopted.

2.2 Computational grid

As mentioned above, the flow is quasi-steady when the flow velocity is perpendicular to the propeller disk. Therefore, only one of the blades needs to be simulated while the influence of other blades can be simulated by the rotational symmetric boundary conditions. In order to simulate the tailing vortex structure and to implement the rotational symmetric boundary conditions, the chimera grid technique is adopted. The chimera grid system used in this article consists of a H-H type background grid and a C-H type blade grid, as shown in Fig. 1 and Fig. 2. The background grids near the proplet are locally refined. Fig. 3 shows the sectional views of the overall grids and grids near the proplet. Fig. 4 is the schematic of hole digging effect when determining the nested relation.

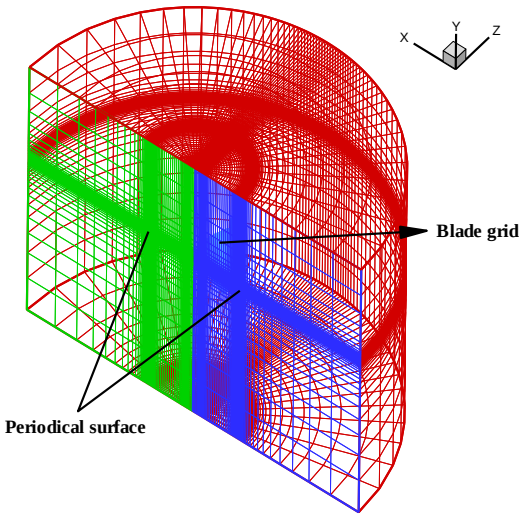

Fig. 1 Schematic diagram of the chimera grid

(a) View A (b) View B

Fig. 2 Schematic of the grid for the propeller with the proplet

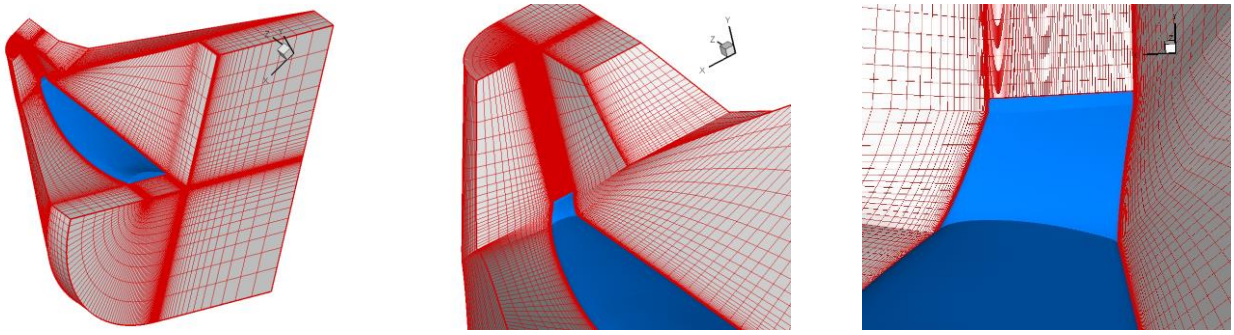

(a) View A (b) View B (c) View C

Fig. 3 Sectional views of the overall grid and grid near the proplet

(a) General schematic diagram (b) Spanwise cross-sectional view

Fig. 4 Schematic diagrams of hole digging effect

2 Parameterization method of the proplets

Fig. 5 shows the general schematic of the proplets studied in this paper. The geometric parameters, which were proposed in literature[7], include: the bending radius r_{let} , the bending angle β_{let} , the incident angle α_{let} of the proplet end surface and the length S_{let} of the proplet linear segment. In addition, this paper introduces the chord length c_{let} of the proplet end surface and the sweep angle Λ_{let} of the proplet , as shown in Fig. 6. Furthermore, the corresponding parameterization program is developed.

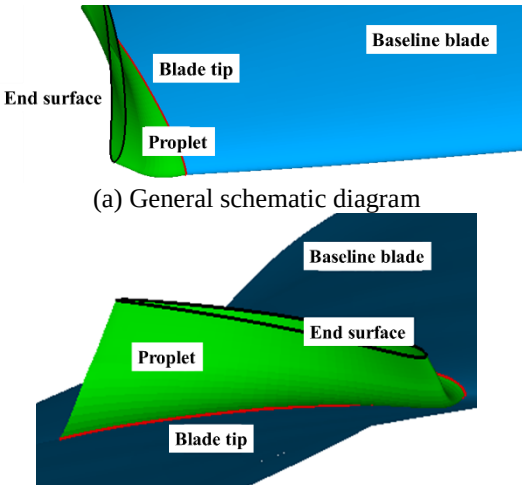

(a) General schematic diagram

(b) Spanwise view

Fig. 5 Schematic diagrams of the proplet

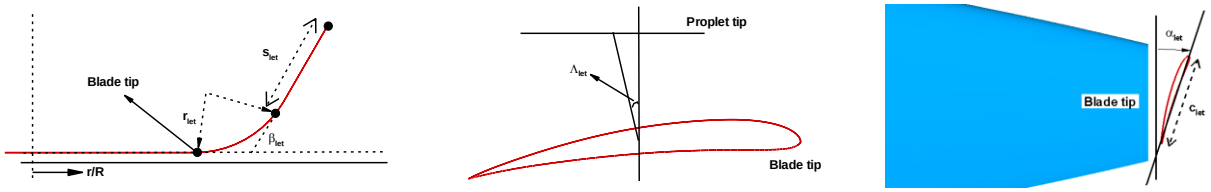

Fig. 6 Schematic diagrams of the geometric parameters for the proplet

3 Power matching method of the propellers

Generally, the absorbed power of the propellers is given, then design parameters such as diameter, rotation speed, distribution of the chord length and twist angle will be adjusted to absorb the given power as much as possible. After the parameters of propeller geometry shape are determined, the speed and pitch angle can be adjusted according to the design requirements to make the propeller absorb the available power as much as possible under the limited torque. According to the characteristics that the propeller absorbed power is varying with the rotation speed and pitch angle monotonically, this paper adopts the Newton iteration method for solving non-linear equations to realize the power matching, and develops a set of power matching method based on Newton iteration. Here takes the varying rotation speed as an example to describe the computing process of this methodology:

The relationship between the power and the power factor is:

$$P_s = C_{Ps}\rho_\infty n_s^3 D^5 \qquad (2)$$

where ρ_∞ is the density of the free-stream, n_s is propeller rotation speed (rev/s), D is the diameter of the propeller. Then the derivative of the power with respect to the rotation speed is:

$$P_s' = \frac{\partial P_s}{\partial n_s} = \frac{\partial C_{Ps}}{\partial n_s}\rho_\infty n_s^3 D^5 + 3C_{Ps}\rho_\infty n_s^2 D^5 \qquad (3)$$

According to the Newton iteration method, we have:

$$n_s(k+1) = n_s(k) - \frac{P_s - P_{s0}}{P_s'} \qquad (4)$$

where P_{s0} is the power needed to be matched, and k is the iterative step number.

In practical applications, the difference method is adopted to calculate the partial derivative. In order to use the first-order backward differential method to calculate the partial derivative, the power at the two rotation speeds needs to be calculated first. The specific implementation steps of the power matching method in this paper are as follows:

First, given an initial rotation speed n_{s1}, the initial power P_{s1} and power factor C_{Ps1} are calculated.

Second, for it is assumed that the required power P_{s0} is matched when the power factor is C_{Ps1}, then the rotation speed n_{s2} can be calculated by formula (2).

Next, according to n_{s2}, the corresponding power P_{s2} and power factor C_{Ps2} are obtained. Then, P_s' is calculated by using the backward differential method and the next iterative rotation speed can be calculated by the formula (4).

The iteration is continued until the difference of the power P_s and P_{s0} are less than the absolute value of the given error ε_{Ps}.

4 Examples and analysis

4.1 Validation of the propeller aerodynamic analysis method

The proposed methodology is validated against the experimental measurements. The experiments are carried out in the propeller test section of the NF-3 low-speed wind tunnel at Northwestern Polytechnical University, as shown in Fig. 7. The experimental model has 2 blades. The atmospheric parameters of the experiment are as follows: the air density $\rho_\infty = 1.109\,kg/m^3$, the atmospheric pressure $P_\infty = 0.97\times10^5\,Pa$. The experimental conditions are as follows: wind speed equals 13m / s, the range of the rotation speed is from 800 to 2500rpm (rev / min). The chord length at the position of 75% span is taken as the reference

length, which is about 0.109 meters, and the range of the Reynolds number is from 2.5×10^5 to 8×10^6. The distribution of the background grid is $121\times149\times113$, and $225\times81\times61$ for the blade grid. Fig. 8 shows that the calculation results agree well with the experimental results, which can validate the effectiveness of the propeller aerodynamic analysis method.

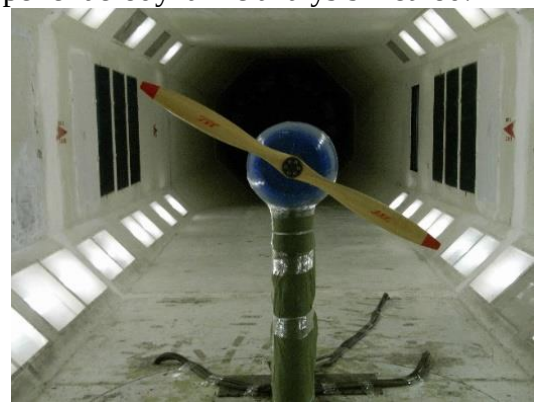

Fig. 7 Propeller model with 1.2m diameter(NF-3 wind tunnel of Northwestern Polytechnical University)

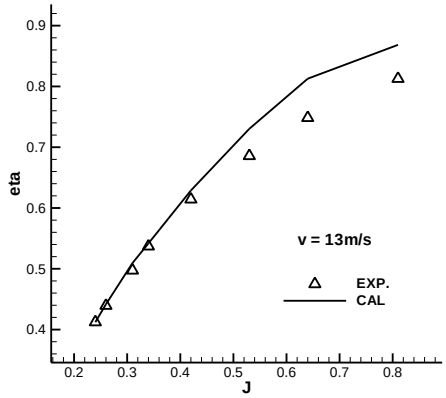

Fig. 8 Calculated and experimental results of the propeller

4.2 Validation of the developed power matching method

To verify the effectiveness of the developed power matching method, a high altitude propeller with a diameter of 6.8m and the design absorbed power of 25.5kw is calculated iteratively using different rotation speeds as the initial rotation speed. The allowable error of the power is 0.1kw, and that means the deviation of the calculated power of the propeller should not larger than 0.4% of the design power. Table 1 shows that the developed power matching method has a high efficiency of iteration. Even if the initial rotation speed has a big difference with the final speed, the calculated power can still converge to the rotation speed corresponding to the given power in the third step.

Table 1 Comparison of the iterative processes with different initial rotation speeds (6.8m diameter, 25.5kw absorbed power)

itera-tive steps	rotation speed (rpm)	power (kw)	rotation speed (rpm)	power (kw)
1	430.0	13.23	530.0	25.98
2	535.2	26.83	526.7	25.45
3	527.0	25.50		

A high altitude propeller with a diameter of 6.2m and the design absorbed power of 2.55kw is also calculated iteratively using different rotation speeds as the initial speed. The allowable error of the power is 0.01kw. Table 2 also indicates that the power matching method is very efficient, even if the initial rotation speed is double of the final speed, the calculated power can still converge to the rotation speed corresponding to the given power in the third step.

Table 2 Comparison of the iterative processes with different initial rotation speeds (6.2m diameter, 2.55kw absorbed power)

itera-tive steps	rotation speed (rpm)	power (kw)	rotation speed (rpm)	power (kw)
1	600.0	21.171	285.0	2.0726
2	296.3	2.3403	305.4	2.5698
3	304.9	2.5572	304.6	2.5500

Take calculations of a propeller with large power and small power for example, the results show that the developed power matching method based on Newton iteration has a high convergent efficiency, and the convergent results are independent of the initial value.

4.3 Aerodynamic characteristics of the high-altitude propellers with proplets

In this section, the research on the configuration of the proplet is conducted in the incompressible flow and compressible flow respectively based on CFD simulation. The mechanism of the influence of the proplets is studied as well.

4.3.1 High-altitude propeller with the 6.2m diameter and 2.55kw absorbed power

The baseline propeller is designed to work at 20km height, the rotation speed is about 300rpm, and the efficiency is 59.85%. The Mach number at the blade tip is about 0.33, therefore the flow is considered as incompressible. In accordance with the general design requirements, the propeller's diameter cannot be too large. Therefore, 97% of the outer part of the propeller is truncated and the proplet is added to ensure the radius of the propeller permanent (the error is smaller than 2mm). The airfoil of the proplet is the same with that of the blade tip. The developed power matching method is used to adjust the speed to make the propeller absorb all the design power.

Table 3 presents the aerodynamic efficiency of the propeller of 20 typical sets of geometric parameters. We can see that the proplets of different geometric parameters can improve the efficiency of the propeller to some extent. When the bending radius is larger than 2%R and the bending angle is greater than 85 degrees, the efficiency can be improved more than 1%. Hence, the propeller is more efficient when the bending angle is close to 90 degrees, which is consistent with the conclusion of literature [7]. The incident angle and the chord of the end surface of the propeller have a great impact on the efficiency, while the sweep angle has little effect. The No.19 configuration reaches the maximum efficiency, which increase from 59.85% up to 61.67%, and the rotation speed is reduced from 304.6 rpm to 275.6 rpm.

Fig. 9 and 10 show the pressure contours and streamlines of the baseline propeller and the propeller with proplet (configuration 19), respectively. The propeller with proplet has a larger area of low pressure on the upper surface, thus it has larger trust and higher efficiency. Fig.11 shows the vorticity iso-surface of the baseline propeller and the propeller with proplet (configuration 19). As we can see, the proplet can weaken the trailing vortex and inhibit the downwash of the wake to some extent, which helps to improve the aerodynamic efficiency.

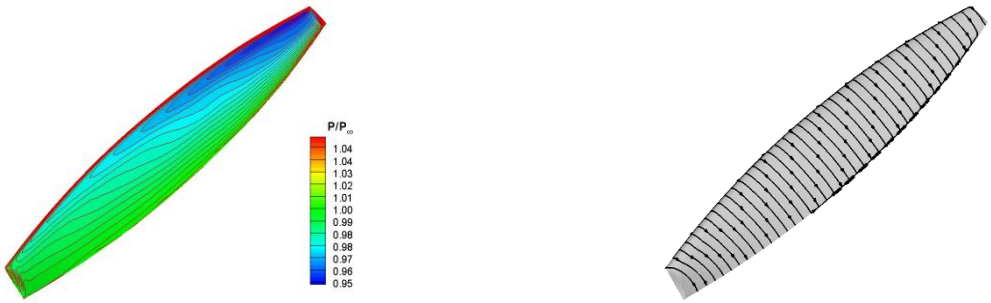

Fig. 9 Pressure contour and streamlines of the baseline propeller (6.2m diameter)

Fig. 10 Pressure contour and streamlines of the propeller with proplet (6.2m diameter)

Table 3 Proplets with different geometric parameters (6.2m diameter, 2.55kw absorbed power)

No.	bending radius r_{let}/R	bending angle $\beta_{let}(\circ)$	length of the proplet linear segment s_{let}/R	incident angle $\alpha_{let}(\circ)$	sweep angle $\Lambda_{let}(\circ)$	chord length c_{let}/R	efficiency $\eta(\%)$	rotation speed $N(rpm)$
baseline propeller	-	-	-	-	-	-	**59.85**	304.6
01	0.0161	76	0.0323	10	0	0.0387	60.35	280.6
02	0.0226	85	0.0258	5	0	0.0387	61.24	278.1
03	0.0081	60	0.0355	5	5	0.0452	60.45	280.2
04	0.0081	60	0.0339	8	0	0.0452	60.43	280.4
05	0.0232	90	0.0661	8	0	0.0419	61.28	275.7
06	0.0232	90	0.0661	8	10	0.0419	61.32	275.8
07	0.0252	90	0.0661	5	0	0.0323	61.58	275.4
08	0.0252	90	0.0661	5	0	0.0258	61.62	275.5
09	0.0265	90	0.0161	0	0	0.0387	61.41	276.9
10	0.0258	90	0.0161	8	10	0.0194	61.42	278.9
11	0.0274	90	0.0065	0	20	0.0194	61.46	278.0
12	0.0274	90	0.0032	5	20	0.0194	61.49	279.2
13	0.0258	88	0.0161	8	0	0.0194	61.33	279.1
14	0.0258	86	0.0161	0	0	0.0194	61.52	278.2
15	0.0252	87	0.0339	0	0	0.0194	61.60	276.8
16	0.0258	88	0.0339	0	0	0.0194	61.61	276.7
17	0.0258	88	0.0258	5	0	0.0194	61.26	278.1
18	0.0252	87	0.0258	6	0	0.0194	61.32	278.3
19	0.0252	89	0.0661	5	0	0.0194	**61.67**	275.6
20	0.0252	89	0.0661	5	0	0.0129	61.63	275.7

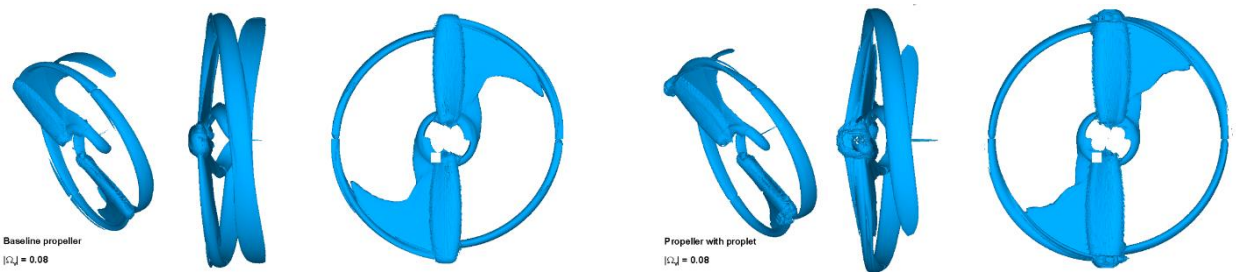

(a)Baseline propeller (b)Propeller with proplet

Fig. 11 Vorticity iso-surface of the baseline propeller and the propeller with proplet (6.2m diameter)

4.3.2 High-altitude propeller with the 6.8m diameter and 25.5kw absorbed power

The baseline propeller is designed to work at 20km height, the rotation speed is about 530rpm, and the efficiency is 44.53%. Under the design condition, the Mach number at the blade tip is 0.64, so the flow of the outer section of the blade is a high subsonic compressible flow. A set of proplet geometric parameters is selected, as shown in Table 4. When the influence of geometric parameters on the propeller efficiency is studied, the other parameters are kept unchanged. According to the previous research, the efficiency of the propeller can be improved when the bending angle is close to 90 degrees, so the bending angle is fixed to 90 degrees in this section.

Fig. 12 shows the effect of the geometric parameters on the aerodynamic efficiency of the propeller. As we can see, the incident angle has the most prominent influence and when it is within 0 to 5 degrees, the efficiency can be improved by 1.2%, while the bending radius has the minimum influence. In addition, the propeller efficiency can be increased slightly with the chord length of the proplet end surface decreasing, or the sweep angle increasing, or the length of the proplet linear segment increasing.

Fig. 13- Fig. 16 show the pressure contours and streamlines of the baseline propeller and the propeller with proplets having different incidence angles. We can see that the flow separation phenomenon exists near the trailing edge on the upper surface of the baseline propeller, while the proplet can effectively restrain the flow separation, although there is still the flow separation existing on the proplet. When the incident angle is -5 degrees, the separation is relatively severe. And when the angle of incidence is 5 degrees, the separation becomes smaller, which is the reason why the efficiency of the propeller is larger when the incident angle is in the range of 0 to 5 degrees. Fig. 17 shows the comparison of the vorticity iso-surface of the base-line propeller and the propeller with proplet at the incident angle of 5 degrees. It is obvious that the propeller with proplets has smaller blade tip vortex, so the efficiency of propeller can be improved.

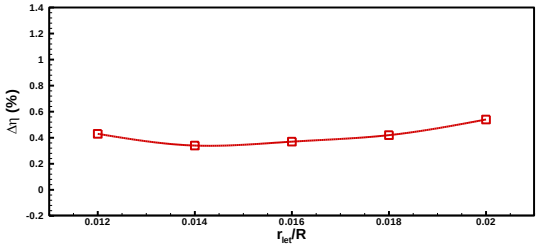

(a) Influence of the bending radius

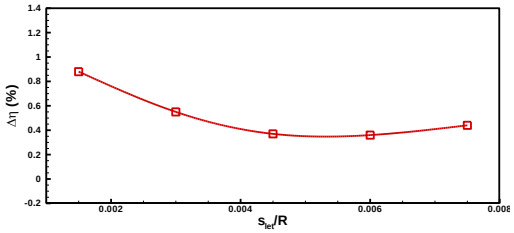

(b) Influence of the length of the proplet linear segment

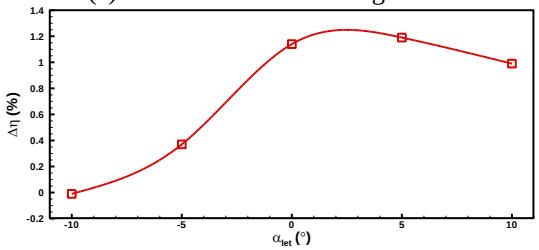

(c) Influence of the incident angle

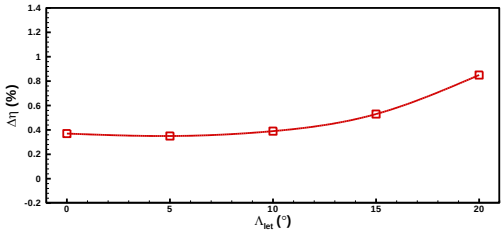

(d) Influence of the sweep angle

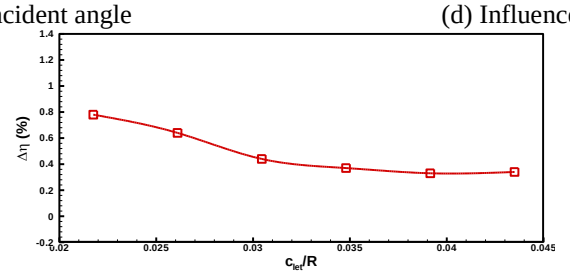

(e) Influence of the chord length of the proplet end surface

Fig. 12 Effect of the geometric parameters on the aerodynamic efficiency of the propeller

Table 4 Baseline geometric parameters of the proplet(6.8m di-ameter, 25.5kw absorbed power)

bending radius r_{let}/R	bending angle $\beta_{let}(\circ)$	length of the proplet linear segment s_{let}/R	incident angle $\alpha_{let}(\circ)$	sweep angle $\Lambda_{let}(\circ)$	chord length c_{let}/R	efficiency $\eta(\%)$
0.016	90	0.0045	-5	0	0.0348	44.90

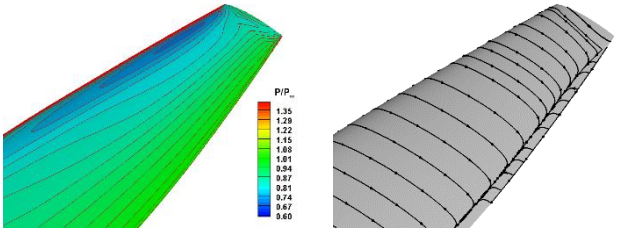

Fig. 13 Pressure contour and streamlines of the baseline propel-ler(6.8m diameter)

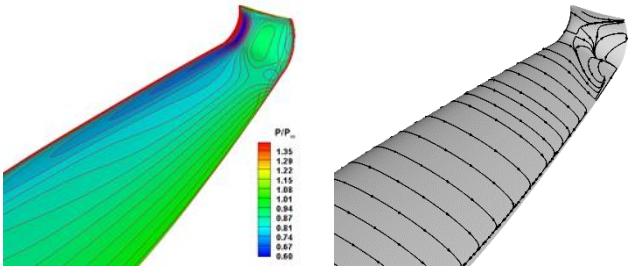

Fig.14 Pressure contour and streamlines of the propeller with proplet(-5 degrees incident angle and 6.8m diameter)

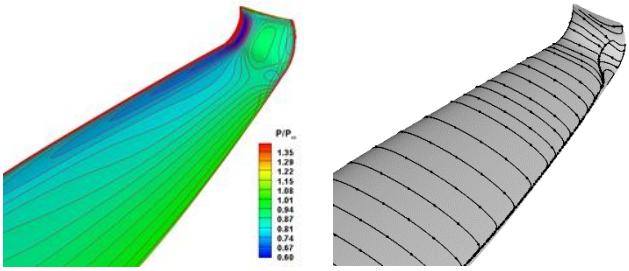

Fig.15 Pressure contour and streamlines of the propeller with proplet(0 degrees incident angle and 6.8m diameter)

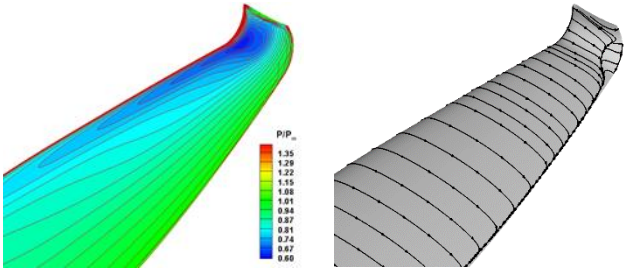

Fig.16 Pressure contour and streamlines of the propeller with proplet(5 degrees incident angle and 6.8m diameter)

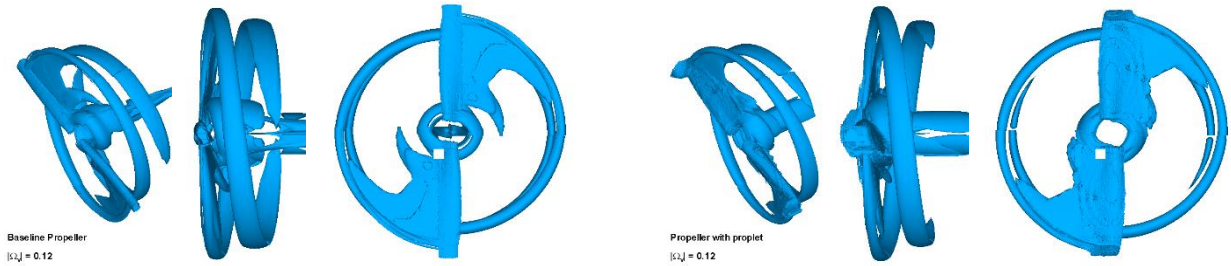

(a)Baseline propeller (b) Propeller with proplet

Fig.17 Vorticity iso-surface of the baseline propeller and the propeller with proplet (6.8m diameter)

5 Conclusions

The proposed Newton-Iteration-based power matching method is very efficient, only two or three steps are needed to reach the required design absorbed power and the convergent result is independent of the initial configuration.

The research results of two propellers with proplets under different design condition show that the incident angle of the proplet has the most influence on the efficiency of the propellers, and it should not be larger than 5 degrees. Only when the bending radius exceeds 2%R, can it improve the efficiency of propellers obviously. It is also benefit to improving the efficiency when the bending angle is close to 90 degrees.

In addition, the study of the sweep angle shows that it has little influence on the efficiency of propellers in the incompressible flow. However, in the compressible flow, the proplet sweep angle is in favor of improving the efficiency of propellers, and larger sweep angle leads to higher efficiency.

References

[1] Zha G C, Carroll B F, Paxton C D, et al. High-Performance Airfoil Using Coflow Jet Flow Control. *AIAA Journal*. Vol. 45, No. 8, pp2087-2090, 2007

[2] Zhu M, Yang X D, Song C, et al. High Synergy Method for Near Space Propeller using Co-Flow Jet Control. *Acta Aeronautica et Astro-nautica Sinica*, Vol. 35, No. 6, pp 1549-1559, 2014.

[3] Cheng Y F, Nie W S. Numerical analysis of the effect of plasma flow control on enhancing the aerodynamic characteristics of stratospheric screw propeller. *Nuclear Fusion and Plasma Physics*, Vol. 32, No. 4, pp 372-378, 2012.

[4] Irwin K., Mutzman R. Propeller Proplet Optimization Based upon Analytical and Experimental Methods. *16th Joint Propulsion Conference*, Hartford, CT, USA, AIAA Paper: 80-1241, 1980

[5] Chang L. K., Sullivan J. P. Optimization of Propeller Blade Twist by an Analytical Method. *AIAA Journal*, Vol. 22, No. 2, pp 252-255, 1984.

[6] Valarezo, W. O. On the Use of Proplets as a Means for Reducing Blade Compressibility Losses. *AIAA 7th Applied Aerodynamics Conference*, Seattle Washington, USA, AIAA Paper: 89-2213, 1989.

[7] Sullivan, J. P., *Proplet Propeller Design/Build/Test Final Report, Purdue University Report*, 2005.

[8] Xu, J. H., Song, W. P., Yang, X. D., Effects of Proplet on Propeller Efficiency. *The 6th International Conference on Fluid Mechanics*, Guangzhou China, 2011.

[9] Xu C J, Yang X D, Zhu M. Aerodynamic Synergistic Mechanism of High Altitude Proplet Propeller Configurations. *Aeronautical Computing Technique*, Vol. 45, No. 5, pp 61-64, 2011.

[10] Xu J H, Song W P, Han Z H, Calculation of Aerodynamic Performance of Propellers at Low Reynolds Number Based on Reynolds-Averaged Navier-Stokes Equations Simulation. *the 5th International Conference on Computational Fluid Dynamics*, Seoul, Korea, 2008.

[11] Xu J H, Song W P, Han Z H, et al A Modified AUSM+-up Scheme for Simulation of Flow around Rotary Blades. *The 52nd Aerospace Sciences Meeting*. National Harbor, Maryland, USA. AIAA-2014-1429, 2014.

[12] Jameson A, Schmidt W, and Turkel E. Numerical solutions of the Euler equations by a finite volume method using Runge-Kutta time stepping schemes. *14th Fluid and Plasma Dynamics Conference*. Palo Alto, CA USA, AIAA Paper:1981-1259, 1981.

[13] Yoon S, Jameson A. Lower-Upper Symmetric-Gauss-Seidel Method for the Euler and Navier-Stokes Equations. *AIAA Journal*, Vol.26, No.9(1988), pp 1025-1026.

[14] Baldwin B, Lomax H. Thin layer approximation and algebraic model for separated turbulent flow. *16th AIAA Aerospace Sciences Meeting*, Huntsville, AL, USA, AIAA Paper 1978-257, 1978.

Copyright Statement